



HAL
open science

Single-fluid MHD model of current-free plasma thrusters with static magnetic fields

P.-Q. Elias, D. Bono

► **To cite this version:**

P.-Q. Elias, D. Bono. Single-fluid MHD model of current-free plasma thrusters with static magnetic fields. 13th ONERA-DLR Aerospace Symposium, May 2013, PALAISEAU, France. hal-01058567

HAL Id: hal-01058567

<https://onera.hal.science/hal-01058567>

Submitted on 27 Aug 2014

HAL is a multi-disciplinary open access archive for the deposit and dissemination of scientific research documents, whether they are published or not. The documents may come from teaching and research institutions in France or abroad, or from public or private research centers.

L'archive ouverte pluridisciplinaire **HAL**, est destinée au dépôt et à la diffusion de documents scientifiques de niveau recherche, publiés ou non, émanant des établissements d'enseignement et de recherche français ou étrangers, des laboratoires publics ou privés.

Single-fluid MHD model of current-free plasma thrusters with static magnetic fields

P.-Q. Elias, D. Bono

ONERA, the French Aerospace Lab, 91123 Palaiseau, France

Abstract: ONERA is involved in the testing and development of new current-free electric thruster (helicon thruster or ECR thruster), using magnetized plasmas. For this development, a numerical tool is desirable to model the magnetized plasma, and assess the overall performances of the system. For this reason, a model for the plasma produced in the thruster has been developed. It boils down to a single-fluid MHD model, where the steady-state solutions, in a static magnetic field, are sought using a finite element approach. First, this model is used to address a simple test problem: the cylindrical vessel, with a purely axial magnetic field. This shows the operation regimes of the discharge: magnetized, non magnetized and a transitional regime. Second, a more realistic thruster configuration is modeled, and the results of the code are used to understand the behavior of the plasma. The strong effect of the magnetic field topology is shown, and in particular the use of a purely diverging magnetic field appears to enhance significantly the performances.

I. Introduction

AS a response to customer needs for lighter satellites, with larger payload, satellite manufacturers start to propose all electric platforms. In these platforms, electric thrusters are used for station-keeping and pointing. As a consequence to this trend, new types of electric thrusters are being considered, in particular to overcome certain limitations of the current flight-proven technologies. Among these new thruster concepts are the current-free magnetically confined thrusters [1], [2]. These thrusters generate and heat a volume of plasma that is magnetically confined. The low pressure plasma is then accelerated to produce thrust. Because the plasma is globally neutral, no net current is drawn from the thruster, hence the term current-free. This is interesting because such device do not require beam neutralization, as it is the case for the current technologies. Beam neutralization relies on hollow cathode neutralizers, which are fragile hardware. Avoiding beam neutralization means an increased robustness and reliability. The helicon thruster is an example of such a current-free thruster [3], [4], [5], [6], [7].

Onera has been involved in the characterization of Helicon-type current-free thrusters [8], and currently develops of new kind of ECR thruster on its own. Both types of thruster involve magnetic confinement with permanent magnets. The confinement is increased because the electrons in the plasma are bound to the magnetic field lines. At low pressure, collisions are infrequent, and thus the electrons cannot diffuse easily across the magnetic stream tubes [9]. Thus, the magnetic field decreases the electron loss rate on the walls of the vessel parallel to the magnetic field lines; this in turn decreases the power requirement to maintain the discharge [10]. Additionally, the magnetic field acts as virtual walls that can shape the plasma, and acts as a nozzle to direct the plasma expansion. So the magnetic field can be tailored to provide magnetic confinement, as well as plasma acceleration.

These magnetically confined plasma sources used for space propulsions pose several theoretical challenges that have been under scrutiny in the last years. For example, the formation of the so-called double layer in the expansion region of the plasma [11], [6], [12] have been investigated using a fluid model of the expanding plasma, assuming the presence of a fraction of hot electrons [13]. The acceleration mechanism of the ions has been investigated, using also fluid models, in [13], [14]. The magnetic confinement in the source has been addressed using fluid approaches [10] and kinetic models [15]. Finally, the problem of the plasma detachment, which is of paramount importance for the overall efficiency of the thruster, has been investigated using various fluid models [16], [17], [18], [19], [20]. To summarize, there are currently three key issues whose understanding is required for the design of an efficient system: 1 the plasma confinement in the source chamber, 2 the acceleration mechanism and 3 the detachment of the plasma from the magnetic stream tubes.

In addition to these three issues, there is currently no numerical tool to properly address realistic thruster assembly. In fact, a key feature of current-free thruster is the use of permanent magnets. The magnetic field topology of these magnets have cusps which are not present on the simpler solenoidal magnetic configuration used in academic research. Furthermore, the complex geometry of the thruster assembly is quite often idealized.

As a consequence, we have sought to develop a fluid model of a current-free thruster with two goals: first, it should implement a plasma model realistic enough to capture the plasma behaviour, in term of confinement, acceleration, and detachment. Second, it should allow us to deal with arbitrary geometries and magnetic configuration, to understand the key parameters influencing the performances of the thruster.

This paper elaborates on the development of this model, and presents some results that have been obtained with it for the study of helicon-type thruster. The first section describes the model, and the numerical method used. The second section presents the analysis of a closed chamber, useful to understand some features of the magnetized plasma. The third section presents the modeling of realistic thruster configuration. Finally, a discussion on the perspective is proposed.

II. Model description

A. Assumptions

In low pressure plasmas, the electron and ion mean free path is usually of the same order or greater than the plasma chamber dimension. In the literature, there are two approaches for the modeling of low pressure magnetized plasma sources. The first is the kinetic method, where electrons, ions and neutrals are described statistically by a population of macro-particles. This yields the so-called Particle In Cell methods [15], [21]. The main advantage of these method is that they derive from first principles; very little macroscopic modeling is required, and only microscopic models are needed. As a consequence, these models accurately capture the non-local effect due to the large electron or ion mean free path. The drawback is that for plasma density high enough, a prohibitively large number of macro-particles is needed to model the plasma. This comes from the fact that PIC method needs, in average, enough particle per mesh cell ; as the plasma density rises, the mesh cell size must be decreased to capture the Debye length scale. Hence, a larger number of cells is needed, which means a larger number of macro-particles.

The second method describes the plasma in a fluid framework. In this case, a set of transport equations, coupled to the Maxwell equations, is used to describe the plasma. Appropriate closure models are required to take into account the collisional effect, or if needed the non-local effects. Depending on the set of assumptions made, this fluid description yields the MHD equations (either ideal or collisional), or a multi-fluid description of the plasma. The advantage of these fluid models is that they can be solved at reasonable computational cost, compared to kinetic model. They can address high-plasma density situation, as well as lower density. The drawback is the need for appropriate closures based on limiting assumption.

In this work, our aim is to model the thruster as a whole to understand the broad factors of influence on the performances. This means that the model must take into account the plasma chamber, and the expansion region, self-consistently. For the purpose of our study, a fluid model of the plasma has been chosen. The reason for this choice mainly comes from the high plasma density in the source ($10^{11} - 10^{12} \text{ cm}^{-3}$), which would require a very expansive PIC simulation in term of computational cost.

For this reason, a fluid model for the plasma produced in the thruster has been developed. First, considering the typical operation parameters of the plasma in the thruster chamber, some simplifying assumptions can be made:

- Axial symmetry
- Quasineutrality: owing to the large plasma density in the chamber, the Debye length is assumed to be small compared to the chamber radius R , which is the characteristic length of the problem $\lambda_D \ll R$. In the asymptotic limit where $\lambda_D \rightarrow 0$, the Poisson equation yields $n_e = n_i = n$, where n_e , n_i and n are the electron, ion and plasma number density.
- Isothermal electrons: This hypothesis derives from the assumption that the electron thermal conductivity is large, and thus that the electron temperature is constant everywhere. This assumption, while used in recent

models ([10], [22]), is currently discussed, in particular in the expanding plume region [23]. Yet there is no clear agreement on this matter. For the sake of simplicity, in this analysis, this assumption of isothermal electrons is retained.

- Local ambipolarity: ions and electrons are supposed to have the same velocity in the r-z plane. However, they do not have the same azimuthal velocity. With this assumption, the meridional current density j is zero everywhere. The ambipolar electric field is such that $j=0$. Note that this hypothesis, assumed in the early works on detachment [16], [24], while still used in some papers [18] is currently debated [22]. In the drift-diffusion limit (ie massless electrons), Bogdanov et al. [25] have shown that local ambipolarity is true as long as $\nabla T_e \times \nabla n = 0$, where n ion-electron number density and T_e is the electron temperature. Thus, for isothermal electrons, in the drift-diffusion limit, this assumption is consistent.
- Plasma production mechanism: the plasma production is modelled with a constant ionization coefficient k_i in the ionization chamber. This is consistent with the isothermal approximation, and it also means that the neutral background is not significantly depleted by the plasma
- Plasma loss mechanism: due to the relatively low pressure in the ionization chamber (a few Pa), volume recombination is unlikely in the chamber and in the expanding plume. The plasma recombines on the walls of the chamber. These walls are made of dielectric material, and thus can draw no current from the plasma. However, a sheath must appear near these walls because the electron and ion flux are equal on the dielectric surface. This sheath cannot be resolved in the present quasi-neutral approximation. However, the formation of the sheath requires that the ions entering the sheath have at least the Bohm velocity[26]. This imposes a condition on the normal velocity of the plasma at the boundaries.

Typical plasma parameters in the source	
Plasma number density n	$10^{17} - 10^{19} \text{ m}^{-3}$
Electron temperature T_e	$\sim 10 \text{ eV}$
Electron to Ion mass ratio	$1.35 \cdot 10^{-5}$
Bohm velocity	$\sim 5000 \text{ m/s}$
Magnetic field	$300 - 1000 \text{ G}$
Chamber neutral pressure	$1e-3 - 1e-2 \text{ mbar}$
Characteristic lengths	
Chamber radius	$\sim 1 \text{ cm}$
Electron mean free path	$5 - 50 \text{ cm}$
Ion mean free path	$2 - 20 \text{ cm}$
Debye length	$\sim 10^{-3} \text{ cm}$
Larmor radius	$\sim 10^{-1} \text{ cm}$
Characteristic times	
Ion transit time	$2 \cdot 10^{-6} \text{ s}$
Ion neutral collision time	$4 \cdot 10^{-6} - 4 \cdot 10^{-5} \text{ s}$
Electron neutral collision time	10^{-7} s
Ionisation time	10^{-5} s
Electron gyroperiod	$3 \cdot 10^{-10} - 10^{-9} \text{ s}$

Table 1 : typical plasma parameters and scales in the thruster (Argon)

B. Model equations

With this set of assumption, the plasma model boils down to a single-fluid MHD model, where the steady-state solutions, in a static magnetic field, are sought. The system of equations consists of a particle balance equation, two momentum transport equation for the plasma, in the axial and radial direction, and an electron momentum transport equation in the azimuthal plane. For the sake of generality, all quantities are dimensionless. Setting:

$$x = x^+ R, \quad y = y^+ R, \quad u = U_0 u^+, \quad v = U_0 v^+, \quad w_e = U_0 w_e^+, \quad \phi = \frac{kT_e}{e} \phi^+, \quad p = n_0 k_B T_e p^+, \quad B = B_0 B^+$$

The reference velocity is chosen so that $U_0^2 = kT_e / M$. The final set of equations is :

$$\frac{\partial n}{\partial t} + \frac{\partial}{\partial x} nu + \frac{\partial}{\partial y} nv + \frac{nv}{y} = Zn \quad (1)$$

$$\frac{\partial nu}{\partial t} + \frac{\partial}{\partial x} nuu + \frac{\partial}{\partial y} nuv + \frac{nuv}{y} = \frac{w_e}{\alpha} nB_y^+ - \frac{\partial n^\gamma}{\partial x} \quad (2)$$

$$\frac{\partial nv}{\partial t} + \frac{\partial}{\partial x} nuv + \frac{\partial}{\partial y} nvv + \frac{nv^2}{y} = -\frac{w_e}{\alpha} nB_x^+ - \frac{\partial n^\gamma}{\partial y} + \frac{\delta n w_e^2}{y} \quad (3)$$

$$\frac{\partial n w_e}{\partial t} + \frac{\partial}{\partial x} nuw_e + \frac{\partial}{\partial y} nvw_e + \frac{2nvw_e}{y} = -\frac{1}{\alpha \delta} n(uB_y^+ - vB_x^+) \quad (4)$$

The electron pressure is expressed by a local closure $p^+ = n^{+\gamma}$. For $\gamma=1$, the electrons are isothermal.

This set of equation is driven by three control parameters:

1. Electron to Ion mass ratio $\delta = \frac{m}{M}$
2. Non-dimensionalized ion larmor radius $\alpha = \frac{r_{Li}}{R} = \frac{MU_0}{eB_0R}$
3. Non-dimensionalized ionization frequency $Z = \frac{k_i n_g R}{U_0}$

The non-dimensionalized ion larmor radius α defines the strength of the magnetic field. The larger α , the weaker the magnetic field. Conversely, for a given magnetic field, the higher the electron temperature is, the larger the reduced ion larmor radius.

The parameters values, corresponding to a helicon-type thruster tested at Onera, are given in Table 2. For some value, where measurements are not available, guess values have been considered.

R	Discharge Radius	9.1 mm (Measured)
U_0	Bohm Velocity, $U_0 = \sqrt{\frac{k_B T_e}{M}}$	4900 m/s
n_0	Maximum plasma density	$1.4 \cdot 10^{18}$ - $1.4 \cdot 10^{20}$ m^{-3} (Guess)
T_e	Electron temperature	10 eV (Guess)
B_0	Maximum magnetic induction on axis	390 G (Measured)
δ	Electron to ion mass ratio	10^{-4} - $1.36 \cdot 10^{-5}$
α	Reduced ion Larmor radius	5.23
M0	Mach number	1

Table 2: Parameters used in the simulation

The maximum plasma density is guessed by considering the neutral pressure in the chamber. For a pressure of 0.58 Pa, the mass flow rate is 0.09 mg/s. This corresponds to a neutral number density (at 300 K) of $1.4 \cdot 10^{20} m^{-3}$. We then assume a 1%-ionization, at 10% and a 100%-ionization, giving a maximum plasma density in the range $1.4 \cdot 10^{18}$ - $1.4 \cdot 10^{20} m^{-3}$.

As can be seen in equation (1), the production of the plasma is due to the volume source term Zn in the particle balance equation. The plasma is lost by two mechanisms:

1. Convection out of the computational domain
2. Surface recombination on the walls.

The two mechanisms are modelled by:

1. A supersonic outlet boundary conditions
2. A sonic velocity normal to the solid walls ($Un = 1$, where Un is the normal velocity), so that the plasma enters the sheath with the Bohm velocity.

C. Resolution strategy

These equations are solved using a finite element scheme, using the Galerkin method. To insure the stability of the scheme, artificial dissipation is added in the equations. The non-dimensional form of the equations becomes:

$$\frac{\partial n}{\partial t} + \frac{\partial}{\partial x} nu + \frac{\partial}{\partial y} nv + \frac{nv}{y} = Zn + \varepsilon \Delta n \quad (5)$$

$$\frac{\partial nu}{\partial t} + \frac{\partial}{\partial x} nuu + \frac{\partial}{\partial y} nuv + \frac{nuv}{y} = \frac{w_e}{\alpha} nB_y^+ - \frac{\partial n^\gamma}{\partial x} + \varepsilon \Delta(nu) \quad (6)$$

$$\frac{\partial nv}{\partial t} + \frac{\partial}{\partial x} nuv + \frac{\partial}{\partial y} nvv + \frac{nv^2}{y} = -\frac{w_e}{\alpha} nB_x^+ - \frac{\partial n^\gamma}{\partial y} + \frac{\delta n w_e^2}{y} + \varepsilon \Delta(nv) \quad (7)$$

$$\frac{\partial n w_e}{\partial t} + \frac{\partial}{\partial x} nuw_e + \frac{\partial}{\partial y} nvw_e + \frac{2nvw_e}{y} = -\frac{1}{\alpha \delta} n(uB_y^+ - vB_x^+) + \varepsilon \Delta(nw_e) \quad (8)$$

This system of equations is in fact an eigenproblem, with Z , the non-dimensional ionization coefficient, the eigenvalue. This eigenvalue is search iteratively by solving the particle conservation equation to yield the equilibrium Z . The process converges to a steady Z value after roughly ten iterations.

The differential operators are linearized, and a steady-state solution is sought using a Newton method [27]. The convergence of the method is checked with the residuals. Convergence is obtained when the residuals drop to machine accuracy.

D. Convergence analysis

The effect of the viscosity and of the mesh size is assessed in the case of a closed chamber with zero magnetic field, as shown in Figure 1. Spatial convergence is satisfactory for mesh size below $h=0.05$, or artificial viscosity below 10^{-3} .

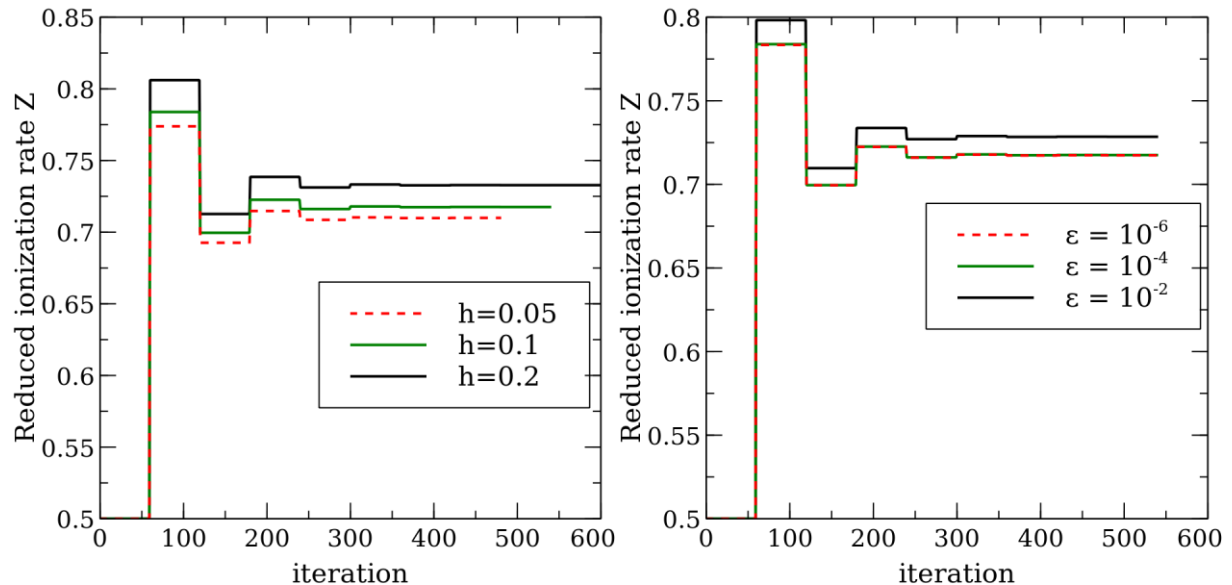


Figure 1. Convergence of the normalized ionization coefficient for different mesh sizes (left) and artificial viscosity (right)

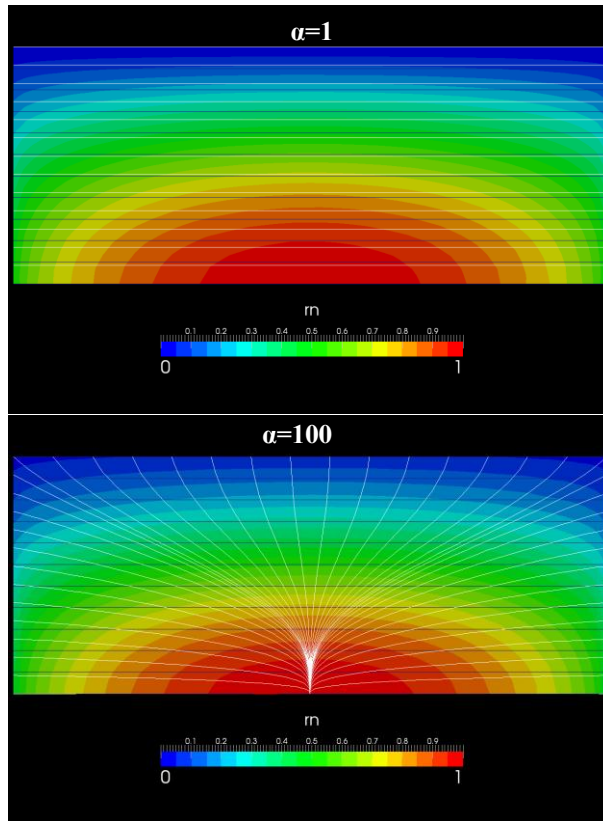
III. Results

A. Closed chamber

As a simplified model, the case of a closed chamber is analyzed. This situation allows to understand the behavior of the plasma in the case of a purely axial magnetic field. The computational domain is a rectangular box. The lower boundary is the axis of symmetry. The three other boundaries are dielectric walls, where the plasma normal velocity is assumed sonic. A constant background of neutral is assumed in the chamber, which is modeled by a uniform ionization coefficient.

As shown in Figure 2, at large magnetic field ($\alpha=1$), the plasma streamlines and the magnetic lines are coincident. The plasma is produced in the volume of the chamber, and is collected to the chamber lateral walls. As the magnetic field decreases, the plasma streamlines are no longer tied to the magnetic lines. More and more plasma is collected on the top wall, as the magnetic confinement decreases.

This behavior is illustrated in the Figure 3, where the non-dimensionalized ionization coefficient is plotted against the reduced ion Larmor radius. For low α , the magnetic field is strong; the plasma is magnetized and well confined along the magnetic field lines. As a consequence, plasma recombines mostly on the lateral walls. Hence, a lower ionization is required to sustain steady-state plasma in the chamber. As α increases, the magnetic field strength decreases (or equivalently the electron temperature increases), and the confinement is less efficient. Some plasma starts to leak on the top wall. A higher ionization is needed to maintain the plasma density. Finally, for higher value of α , an asymptotic regime is reached, in which the plasma no longer feels the effect of the magnetic confinement.



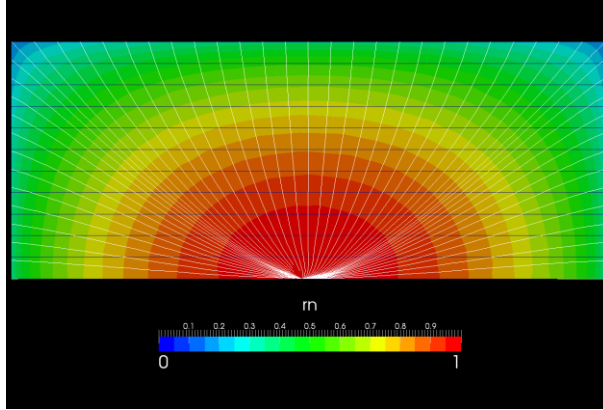


Figure 2. Normalized plasma density, for $\alpha = 1, 100$ and $100\,000$. The black lines are the magnetic field lines, the white ones are the plasma streamlines

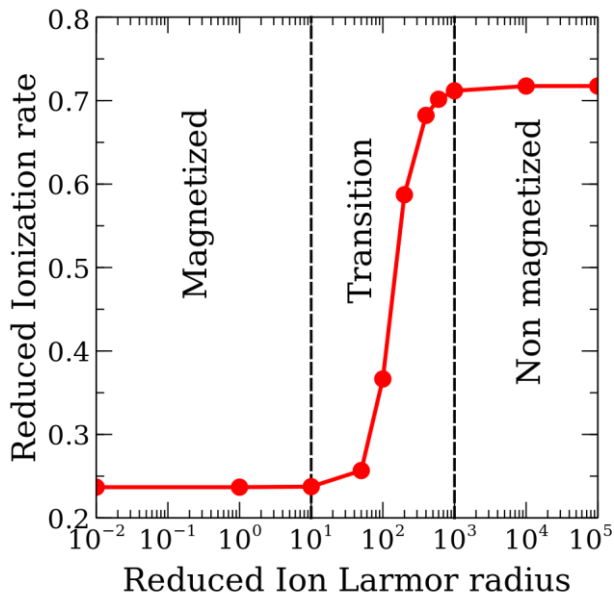


Figure 3: Effect of magnetic field on the ionization rate required to maintain the discharge

B. Open chamber

The case of the closed chamber is helpful to understand the behaviour of the plasma in the case of a realistic geometry, as shown in Figure 4. A uniform volume ionization is prescribed in the thruster chamber only. A solid nozzle allows the plasma to expand in vacuum. Supersonic outlet boundary conditions are prescribed on the top right boundary conditions.

The magnetic topology used in this case is no longer a simple axial field. The field is the one produced by an arrangement of cylindrical permanent magnets. The field is axisymmetrical, and is shown in Figure 5. Its peculiarity is the presence of two cylindrical cusps on the magnet, and two points where a field inversion occurs (zero crossing),

along the symmetry axis. This magnet arrangement can be moved around the thruster chamber, so the position of the zero crossing can be changed to be in or out of the plasma chamber, as described in Table 3.

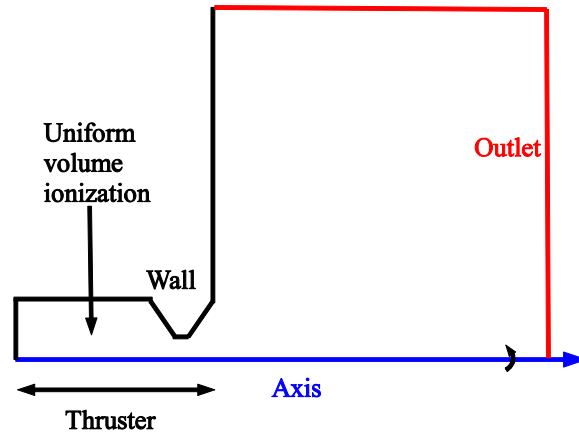


Figure 4. Computational domain for the thruster geometry

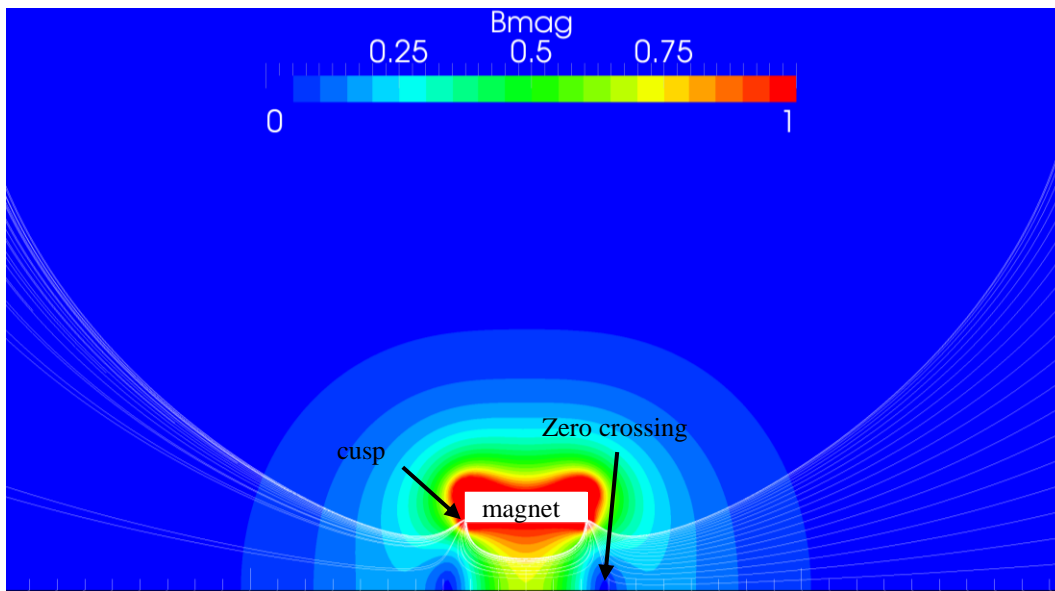


Figure 5: View of the magnetic field around the permanent magnet

Case	Magnet position	Geometry	α
0	NA	Chamber with endplate	∞
1	Zero crossing in chamber	Chamber with endplate	5.27
2	Zero crossing outside chamber	Chamber with endplate	5.27
3	Zero crossing in chamber	Short chamber, no endplate	5.27
4	Coil	Chamber with endplate	5.27
5	Zero crossing before chamber	Short chamber, no endplate	5.27

Table 3. Test cases description

In Figure 6, a qualitative comparison between the shape of the plume observed and the plasma density computed with the model, for the test case 2. The plasma emission can be thought to be related to the plasma number density.

The features observed in the experiment are also found in the model. The plasma expands through a narrow axial jet, while it also expands radially to reach the cusp on the permanent magnet. In Figure 7, the plasma streamlines in the chamber and in the expansion region are shown. It appears that a significant fraction of the plasma going through the solid nozzle is channeled to the cusp region when reaching the zero crossing region. Overall, this acts as a filter, that forces back a part of the expanding plasma towards the thruster. As a consequence, this part of the plasma does not contribute to the overall thrust.

Several test cases have been considered, and the performance parameters derived from the computations are shown in Table 4. The first parameter is called η_I , it compares the current going out of the source, in the plume, to the total charge flux in the source (related to the volume ionization). The second parameter, called η_T , compares the actual thrust to the thrust obtained if the plasma were not diverging. This latter "ideal" thrust is defined as the total momentum leaving the computational domain. That parameter measures the divergence of the beam. The third performance parameter η_P compares the power dissipated in the outgoing plasma plume to the total power deposited in the thrusters. (ie collected on the walls + outgoing).

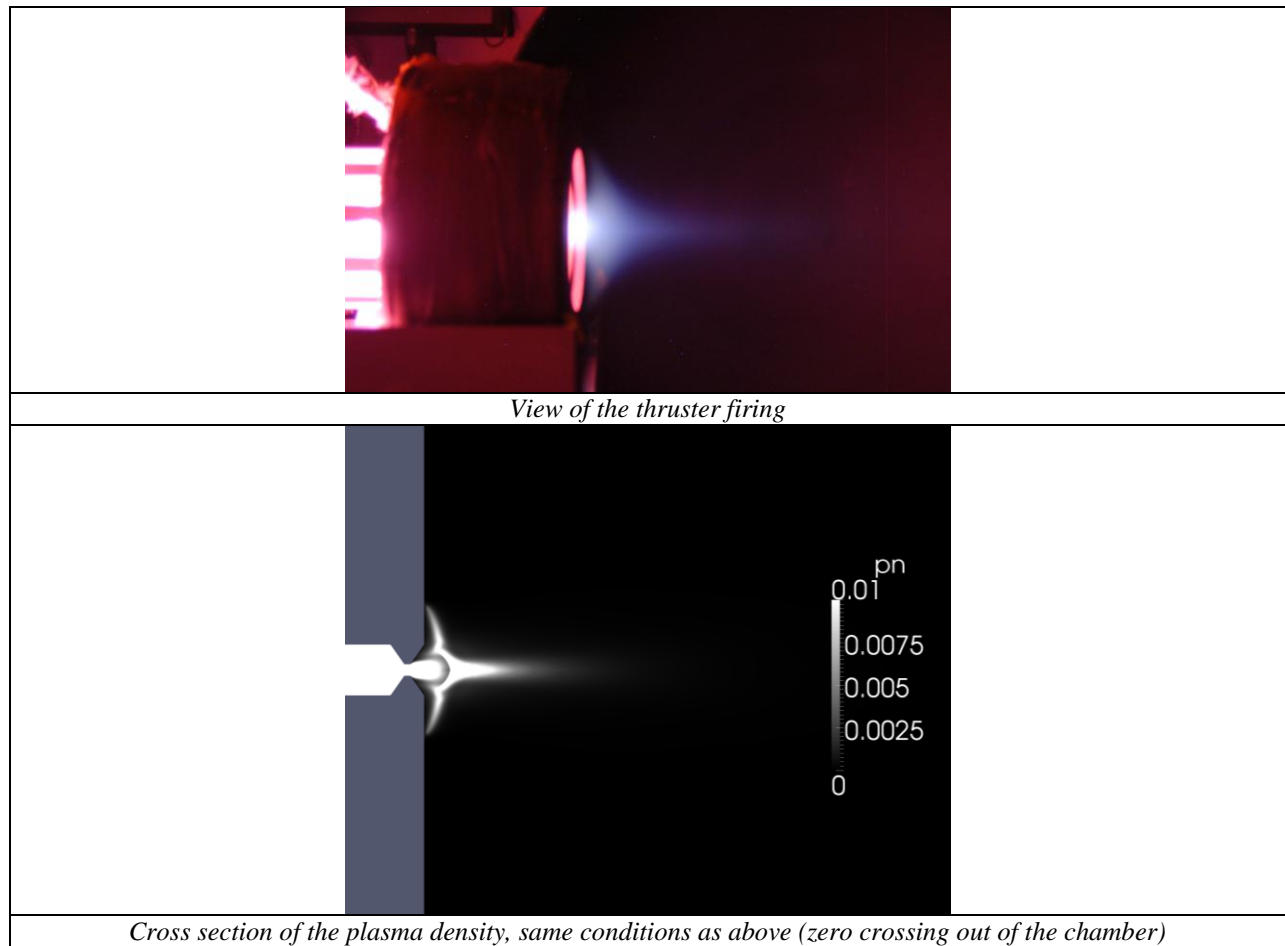


Figure 6: Qualitative comparison of the plume shape

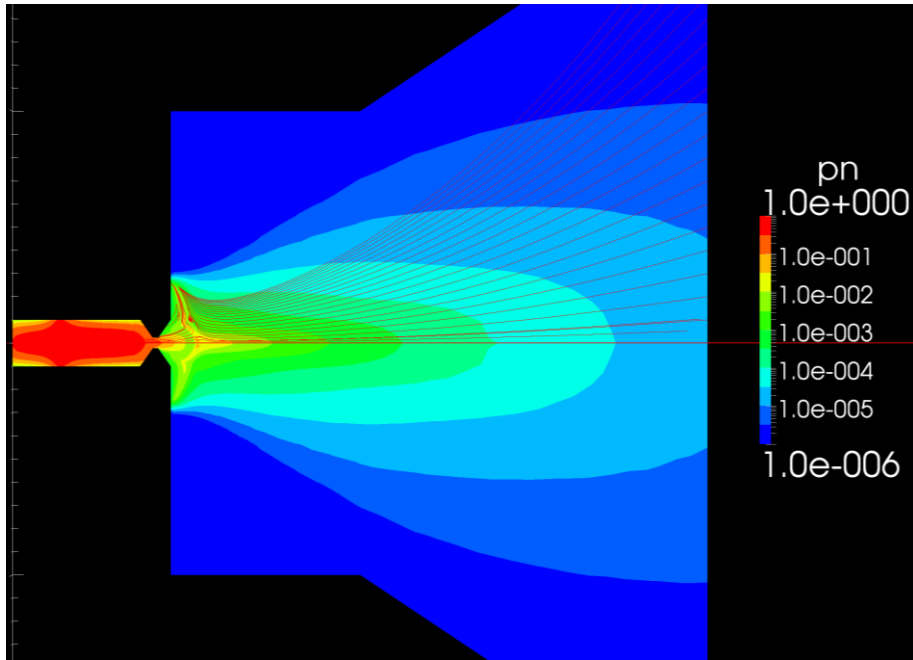


Figure 7: Case 2, density field. Plasma streamlines are also shown in the upper half only (red)

Test Case	Power Efficiency η (mN/kW)	Outgoing current ratio η_I	Outgoing power ratio η_P	Thrust to ideal thrust ratio η_T
0	0.12 mN/kW	0.07 %	0.48 %	61 %
1	0.75 mN/kW	0.42 %	1.63 %	88.5 %
2	0.60 mN/kW	0.44 %	1.26 %	88.0 %
3	1.25 mN/kW	0.79 %	2.47 %	80.1 %
4	1.37 mN/kW	0.78 %	3.57 %	80.0 %
5	36.8 mN/kW	32.6 %	58.4 %	92.0 %

Table 4: Performance parameters

First, we note that the case with no magnetic field has the worst performances. This is so because the plasma is not confined in the source by the field. As a result, power losses on the wall are greater, and the beam diverges dramatically while expanding in vacuum.

Second, we see that case 2, while allowing more current to flow through the endplate, has a lower thrust, because less power is deposited in the plasma jet. Indeed, the plasma Mach number is lower in this configuration than in configuration 1.

Finally, in configuration 3, the power losses are reduced, because of the smaller chamber, and better confinement in the diverging part of the magnetic field. Also, the removal of the endplate prevents large power loss at this surface.

While the beam diverges more than the cases 1 and 2 (η_T is greater), the power deposited in the beam is greater. However, most of the current flows back to the thrusters, because of the cusp. Overall, the typical thrust in this configuration is close to the cases 1 and 2, however the power efficiency is better

The most favourable case is the one where the magnetic field is purely diverging (case 5). When the zero crossing is placed upstream of the plasma chamber, the chamber and the expansion region, are located in the purely diverging region of the magnetic field. In this case, the whole plasma is expanding; no fraction of it is redirected to the thruster walls in the cusp region. As a consequence, while less than 1% of the plasma current actually leaves the thrusters when the cusp is in or downstream of the chamber (with the endplate), as much as one third of the plasma current leaves the chamber and thus contributes to the total thrust. This is illustrated in Table 4, where the thrust to power ratio in case 5 is well above the other configurations. To get hindsight on the actual performances of these thruster

configurations, the ion current, thrust and power are given in Table 5. Using the momentum balance equations (2), the thrust is shown to be:

$$T_x = \underbrace{\int_{\Omega_0} e w_e n_i B_y^+}_{\text{Magnetic}} - \underbrace{\int_{\Sigma_T} M n_i (u \bar{u} \cdot \bar{n} + p n_x)}_{\text{Kinetic}} dS$$

With a kinetic contribution due to the plasma flux on the wall, and a magnetic contribution, due to the formation of electron azimuthal currents in the plasma plume.

5 % ionization, $n_0=7 \cdot 10^{18} \text{ m}^{-3}$				
Test Case	Power required (W)	Current through endplate (mA)	Plume current (mA)	Thrust (μN)
0	233.0 W	12,1 mA	4,5 mA	29 μN
1	60.8 W	15,2 mA	5,7 mA	45 μN
2	59.7 W	26,0 mA	5,9 mA	35 μN
3	35.5 W	331,5 mA	6,2 mA	44 μN
4	46.3 W	16.8 mA	8.0 mA	63 μN
5	50.5 W	300.4 mA	252 mA	1864 μN

Table 5: Current, power and thrust, assuming 5% ionization

IV. Conclusion and future work

In this paper, a model is presented to study the behavior of current-free quasi-neutral plasma thrusters. It consists of a single-fluid MHD model with a static magnetic field. The model is used on the simple case of a closed chamber, with constant neutral background density, and axial magnetic field. This illustrates the ability of the magnetic field to confine the plasma, thereby decreasing the wall loss and the power requirement of the discharge. In a second step, several cases are treated to represent a thruster configuration tested at Onera. The results of the model and the experiments agree qualitatively. This agreement needs to be further confirmed through dedicated experiments. The model demonstrates the strong effect of the magnetic topology on the thruster performances. In particular, the cusp regions are shown to act as a filter that channel part of the exiting plasma back to the thruster wall. For this reason a purely diverging topology seems more appropriate.

Several key issues remain for the numerical modeling of that kind of thruster. First, the effect of the boundary needs to be addressed. In the real system, the plasma chamber wall can be dielectric, floating conductors or grounded conductors. This may have an importance in the self-biasing process of the plasma chamber and thus on the overall performance of the thruster. Second, the effect of neutral depletion is neglected in the model. For high density plasmas, the neutral gas can be significantly depleted; this alters the ionization rate uniformity. Third, in the expansion region, the assumption of local ambipolarity made in the model might force a premature plasma detachment. Electron inertia may play an important role and thus needs to be taken into account. For this reason, future work will extend our modeling effort to tackle these issues, using in particular a 2-fluid MHD code.

References

- [1] C. Charles, « Plasmas for spacecraft propulsion », *J. Phys. Appl. Phys.*, vol. 42, n° 16, p. 163001, 2009.
- [2] J. C. Sercel, « An experimental and theoretical study of the ECR plasma engine », CalTech, 1993.
- [3] O. Batishchev et J.-L. Cambier, « Experimental Study of the Mini-Helicon thruster », févr. 2009.
- [4] O. V. Batishchev, « Minihelicon Plasma Thruster », *Ieee Trans. Plasma Sci.*, vol. 37, n° 8, p. 1563-1571, 2009.
- [5] R. W. Boswell, « Very efficient plasma generation by whistler waves near the lower hybrid frequency », *Plasma Phys. Control. Fusion*, vol. 26, n° 10, p. 1147 -1162, 1984.
- [6] C. Charles et R. W. Boswell, « Current-free double-layer formation in a high-density helicon discharge », *Appl. Phys. Lett.*, vol. 82, p. 1356-1358, 2003.

- [7] M. Wiebold, Y.-T. Sung, et J. E. Scharer, « Experimental observation of ion beams in the Madison Helicon eXperiment », *Phys. Plasmas*, vol. 18, n° 6, p. 63501, 2011.
- [8] D. Pavarin, F. Ferri, M. Manente, A. Lucca Fabris, M. Faenza, F. Trezzolani, L. Tassinato, O. Tudisco, A. Lohan, Y. Protsan, et others, « Thruster development set-up for the helicon plasma hydrazine combined micro research project », in *Proceedings of the 32nd International Electric Propulsion Conference (IEPC'11)*, 2011.
- [9] F. F. Chen, *Introduction to plasma Physics*. Plenum Press, 1977.
- [10] E. Ahedo, « Parametric analysis of a magnetized cylindrical plasma », *Phys. Plasmas*, vol. 16, n° 11, p. 113503, 2009.
- [11] G. Hairapetian et R. L. Stenzel, « Particle dynamics and current-free double layers in an expanding, collisionless, two-electron-population plasma », *Phys. Fluids B Plasma Phys.*, vol. 3, n° 4, p. 899-914, 1991.
- [12] S. C. Thakur, A. Hansen, et E. E. Scime, « Threshold for formation of a stable double layer in an expanding helicon plasma », *Plasma Sources Sci. Technol.*, vol. 19, n° 2, p. 025008 (10pp), 2010.
- [13] E. Ahedo et M. Mart, « The Role Of Current-Free Double-Layers In Plasma Propulsion », n° July, 2008.
- [14] A. V. Arefiev et B. N. Breizman, « Ambipolar acceleration of ions in a magnetic nozzle », *Phys. Plasmas*, vol. 15, p. 042109, 2008.
- [15] S. Kolev, G. J. M. Hagelaar, G. Fubiani, et J.-P. Boeuf, « Physics of a magnetic barrier in low-temperature bounded plasmas: insight from particle-in-cell simulations », *Plasma Sources Sci. Technol.*, vol. 21, n° 2, p. 25002, 2012.
- [16] E. B. Hooper, « Plasma detachment from a magnetic nozzle », *J. Propuls. Power*, vol. 9, n° 5, p. 757-763, 1993.
- [17] B. N. Breizman, M. R. Tushentsov, et A. V. Arefiev, « Magnetic nozzle and plasma detachment model for a steady-state flow », *Phys. Plasmas*, vol. 15, p. 057103, 2008.
- [18] P. F. Schmit et N. J. Fisch, « Magnetic detachment and plume control in escaping magnetized plasma », *J. Plasma Phys.*, vol. 75, n° 03, p. 359-371, 2009.
- [19] E. Ahedo et M. Merino, « On plasma detachment in propulsive magnetic nozzles », *Phys. Plasmas*, vol. 18, n° 5, p. 53504, 2011.
- [20] A. V. Arefiev et B. N. Breizman, « Magnetohydrodynamic scenario of plasma detachment in a magnetic nozzle », *Phys Plasmas*, vol. 12, n° 4, p. 043504, 2005.
- [21] R. Gueroult, P. Q. Elias, D. Packan, J. Bonnet, et J. M. Rax, « Particle in cell modelling of the observed modes of a dc wire discharge », *J. Phys. Appl. Phys.*, vol. 43, n° 36, p. 365204, 2010.
- [22] E. Ahedo et M. Merino, « Two-dimensional supersonic plasma acceleration in a magnetic nozzle », *Phys. Plasmas*, vol. 17, n° 7, p. 073501, 2010.
- [23] A. V. Arefiev et B. N. Breizman, « Collisionless plasma expansion into vacuum: Two new twists on an old problema... », *Phys. Plasmas*, vol. 16, p. 055707, 2009.
- [24] H. G. Kosmahl, « Three-dimensional plasma acceleration through axisymmetric diverging magnetic fields based on dipole moment approximation », 1967.
- [25] E. A. Bogdanov, A. S. Chirtsov, et A. A. Kudryavtsev, « Fundamental Nonambipolarity of Electron Fluxes in 2D Plasmas », *Phys Rev Lett*, vol. 106, n° 19, p. 195001, mai 2011.
- [26] J. E. Allen, « The Plasma Boundary in a Magnetic Field », *Contrib. Plasma Phys.*, vol. 48, n° 5-7, p. 400-405, 2008.
- [27] P. Meliga, D. Sipp, et J. M. Chomaz, « Open-loop control of compressible afterbody flows using adjoint methods », *Phys. Fluids*, vol. 22, p. 054109, 2010.